Molecular Vision 2016; 22:886-897 <http://www.molvis.org/molvis/v22/886>
Received 24 January 2016 | Accepted 22 July 2016 | Published 25 July 2016

Tissue factor induces VEGF expression via activation of the Wnt/β-catenin signaling pathway in ARPE-19 cells

Ying Wang, Aimin Sang, Manhui Zhu, Guowei Zhang, Huaijin Guan, Min Ji, Hui Chen

(The first three authors contributed to this work equally.)

Eye Institute, Affiliated Hospital of Nantong University, Nantong, Jiangsu, China

Purpose: The purpose of the present study was to investigate the potential signal mechanism of tissue factor (TF) in the regulation of the expression of vascular endothelial growth factor (VEGF) in human retinal pigment epithelial (ARPE-19) cells.

Methods: An in vitro RPE cell chemical hypoxia model was established by adding cobalt chloride ($CoCl_2$) in the culture medium. The irritative concentration of $CoCl_2$ was determined with a 3-(4,5-dimethylthiazol-2-yl)-2,5-diphenyl tetrazolium bromide (MTT) assay kit. VEGF production in ARPE-19 cells was measured with enzyme-linked immunosorbent assay (ELISA) and western blotting. The Wnt signaling pathway–associated molecules, including phospho-glycogen synthase kinase 3β (p-GSK3β), GSK3β, p-β-catenin and β-catenin, were detected with western blotting. pEGFP-N3-hTF was constructed and verified with digestion of the restriction enzyme and sequencing analysis. Human TF overexpression and silencing plasmids were transfected into the ARPE-19 cells to clarify the causal relationship between TF and VEGF expression. The Transwell coculture system of ARPE-19 cells and RF/6A rhesus macaque choroid–retinal endothelial cells was performed to evaluate cell invasion and tube formation ability.

Results: Our anoxic model of ARPE-19 cells showed that TF expression was upregulated in accordance with variations in hypoxia-inducible factor 1-alpha (HIF-1α) and VEGF levels. Silencing and overexpression of TF decreased and increased VEGF expression, respectively. The Wnt/β-catenin signaling pathway played an important role in this effect. Results from the ARPE-19 cell and RF/6A cell coculture system showed that the enhancement of TF expression in the ARPE-19 cells led to significantly faster invasion and stronger tube-forming ability of the RF/6A cells, while siRNA-mediated TF silencing caused the opposite effects. Pharmacological disruption of Wnt signaling IWR-1-endo inhibited the effects compared to the TF-overexpressing group, indicating the importance of the Wnt/β-catenin signaling pathway in the process of TF-induced VEGF expression and angiogenesis.

Conclusions: Involvement of the activation of the Wnt/β-catenin signaling pathway is an important mediator for TF-induced VEGF production during the process of angiogenesis. Thus, our findings may ascertain the molecular regulation of TF in neovessel formation and show significant therapeutic implications.

Age-related macular degeneration (AMD) is the leading cause of blindness among the elderly in developed countries [1]. Wet AMD is characterized by choroidal neovascularization (CNV) beneath the macula, which occurs at the end stage of AMD. The process of CNV formation involves immature new blood vessels penetrating Bruch's membrane from choriocapillaries and extending into the sub-retinal or sub-RPE space [2]. It is known that vascular endothelial growth factor (VEGF) plays a pivotal role in CNV formation [3] and is mainly produced by RPE cells. Oxygen deprivation, inflammation, and other stimuli induce the expression of VEGF and promote the development of CNV. Targeting the proangiogenic factor VEGF has been validated in patients with CNV [4,5]. However, one-sixth of treated patients still progress to legal blindness [6]. Thus, treatment strategies based on more specific targeting of CNV are desirable.

Tissue factor (TF), a 47 kDa transmembrane cell-surface receptor for plasma coagulation factor VII (FVII) and its activated form FVIIa, is the principal initiator of the extrinsic coagulation pathway [7]. In addition to a role in thrombosis, TF has proangiogenic properties, as previous studies showed that TF was one of the key mediators in physiologic and pathological neovascular formation [8-10]. Enhanced expression of TF was observed in the human wet AMD retina compared with the non-AMD retina [8]. TF contributed to the pathologies of AMD by regulation of inflammation [8,11-13], oxidative stress [14-16], and angiogenesis [11,17]. TF is found to be connected to the upregulation of VEGF expression in human patients with astrocytoma [18].

We recently reported that TF siRNA could inhibit endothelial cell proliferation, migration, and tube formation in an in vitro model of neovascularization [19]. We also found that

Correspondence to: Hui Chen, Eye Institute, Affiliated Hospital of Nantong University, Nantong, Jiangsu, China, 226001; Phone: +86 13809082586; FAX: +86 513 85519820; email: chenhuieye@126.com

suppression of TF by intravitreal injection of anti-TF monoclonal antibody significantly ameliorated CNV and decreased the expression of VEGF in the mouse CNV model. The VEGF levels of the RPE–choroid complexes and the retina showed a similar change with TF [20]. However, potential signaling pathways related to the effect of TF on the production of VEGF remain poorly defined.

The canonical Wnt/β-catenin axis is an evolutionarily conserved signaling pathway, which is activated by the Wnt ligand and plays a critical role in the regulation of inflammation and angiogenesis [21]. When activated, β-catenin escapes from serine and threonine phosphorylation by glycogen synthase kinase 3β (GSK3β) at the N-terminus that dictates the stability of the destruction complex [22,23]. Consequently, β-catenin accumulates in the cytoplasm and translocates into the nucleus, regulating the expression of the Wnt target genes [24,25]. Multiple proangiogenic mediators such as VEGF are known Wnt targets, whose promoters contain β-catenin response elements. It has been found that a T cell factor 4 (TCF-4) binding element at −805 bp upstream of the transcriptional start site in the VEGF promoter is an important mediator of this effect [26,27].

In the present study, we found that the Wnt signaling pathway was activated in the in vitro model of RPE cell chemical hypoxia. Overexpression of human TF upregulated the activation of Wnt family members. It can thus be hypothesized that TF regulates the production of VEGF through the Wnt/β-catenin signaling pathway.

METHODS

Cell culture: The ARPE-19 and RF/6A cell lines were purchased from American Type Culture Collection (ATCC, Manassas, VA) and were maintained in RPMI 1640 supplemented with 10% fetal bovine serum (FBS; Gibco, Rockville, MD) and 100 U/ml penicillin-streptomycin mixture (Gibco) at 37 °C in 5% CO_2. The culture medium was changed every 2 days. An in vitro RPE cell chemical hypoxia model was established by adding cobalt chloride ($CoCl_2$) to the culture medium, and cells were harvested after 6, 12, 18, and 24 h. Data from cells cultured without $CoCl_2$ were regarded as normal controls. Inhibition of the Wnt signaling pathway was performed by adding IWR-1-endo (Santa Cruz Biotech, Santa Cruz, CA, CAS 1,127,442-82–3) to a final concentration of 10 μM. IWR-1-exo (Santa Cruz Biotech, CAS 1,127,442-87–8) was used as a control because it has little effect on the Wnt pathway at 10 μM compared with the active form IWR-1-endo. The analysis was conducted within five passages of the cells used in the experiments.

STR analysis: Nineteen short tandem repeat (STR) loci plus the gender-determining locus, amelogenin, were amplified using the commercially available EX20 Kit from AGCU (Wuxi, China). The cell line sample was processed using the ABI Prism® 3500 Genetic Analyzer. Data were analyzed using GeneMapper® ID-X v1.2 software (Applied Biosystems, Suzhou, China). Appropriate positive and negative controls were run and confirmed for each sample submitted. The STR analyses are presented in Appendix 1.

MTT assay: The viability of ARPE-19 cells after the $CoCl_2$ addition was determined with a 3-(4,5-dimethylthiazol-2-yl)-2,5-diphenyl tetrazolium bromide (MTT) assay kit (Beyotime Biotechnology, Shanghai, China). The cells were incubated in 96-well culture plates (Corning, Corning, NY) at a concentration of 1×10^4 cells/well. Various concentrations of $CoCl_2$ (0, 50, 100, 200, and 300 μM) were added into the culture medium. At the end of each time point (6, 12, 18, 24, and 48 h), 20 μl of 5 mg/ml MTT (Sigma, St. Louis, MO) was added to each well for 4 h. Then the supernatant was discarded, and 150 μl dimethyl sulfoxide (DMSO) was administered for 10–15 min. The absorbance was recorded at 570 nm with a Microplate Reader (Model 680, Bio-Rad, City, CA). Each experimental condition was performed in triplicate.

Western blotting: Western blot analysis of ARPE-19 cell lysates was performed as usual [19]. For protein detection, antibodies against TF (RD Systems, Minneapolis, MN), hypoxia-inducible factor 1-alpha (HIF-1α; Chemicon, Temecula, CA), VEGF (Santa Cruz Biotech, Santa Cruz, CA), phosphorylated as well as total β-catenin (Santa Cruz Biotech), glyceraldehyde 3-phosphate dehydrogenase (GAPDH; Sigma Aldrich, Saint Louis, MO), and phosphorylated and total GSK3β (Cell Signaling Technology, Danvers, MA) were used. Protein samples were separated with sodium dodecyl sulfate–polyacrylamide gel electrophoresis (SDS–PAGE) gel and transferred onto polyvinylidene difluoride (PVDF) membranes (Millipore, Bedford, MA). After blocking in 5% nonfat milk at 37 °C for 1 h, the membranes were incubated overnight at 4 °C with primary antibodies. The membranes were then incubated with horseradish peroxide (HRP)–conjugated secondary antibody (Thermo Scientific, Rockford, IL) at 1:2,500 dilution for 2 h at room temperature (RT). The blots were then incubated with chemifluorescent reagent enhanced chemiluminescence (ECL; Thermo Scientific, Rockford, IL) and exposed to X-ray film in the dark. The experiments were performed in triplicate, and the protein bands were quantitatively analyzed with Image J Analysis software.

Enzyme-linked immunosorbent assay: The cell culture media were collected at different treatment time points, centrifuged at 250 ×*g* to remove debris, and frozen until further analysis.

VEGF concentrations were determined using a quantitative enzyme-linked immunosorbent assay (ELISA; Cusabio Biotech Co, Wuhan, China). The amount of VEGF immunoreactivity was calculated using recombinant human VEGF standards present on each microtiter plate. Optical densities were determined at 450 nm using an ELISA reader (Model 680, Bio-Rad, Albany, NY).

Plasmid construction: For transfection experiments, the plasmid pEGFP-N3 (Becton Dickinson, Heidelberg, Germany) was used. A cDNA construct of human full-length TF was cloned into the multiple cloning site of the plasmid with the PCR method. The DNA fragments were inserted into BamHI and KpnI of pEGFP-N3. The quality, orientation, and identity of the construction (pEGFP-N3-hTF) were confirmed with digestion of the restriction enzyme and sequencing analysis. The empty plasmid (pEGFP-N3) was used as control.

Transfections: A total of 2×10^6 ARPE-19 cells per well were seeded in six-well plates and allowed to grow overnight. Transfection of pEGFP-N3-hTF or pEGFP-N3 was performed using Lipofectamine™ 2000 (Invitrogen, Carlsbad, CA) following the manufacturer's protocol. Briefly, for six-well plates, 4 µg DNA was mixed with 10 µl Lipofectamine 2000™ at a final concentration of 2 µg DNA/ml, dissolved in RPMI 1640 without serum, the resulting complex was incubated at for 20 min to generate the transfection mixture and was added to the cells, which were then incubated for 4 to 6 h. Next, the cells were washed with RPMI 1640 and incubated in RPMI 1640 with 10% FBS for a further 48 h until use. The transfection efficiency was higher than 80%, using fluorescence microscopy, with little toxicity visible under a light microscope.

Gene silencing was performed using siRNA against human TF or a scrambled oligonucleotide sequence provided by Santa Cruz, following the manufacturer's instructions. After transfection for 48 h, the cells were collected to perform western blotting.

In vitro cell invasion assay: To test the effect of ARPE-19 cells on the invasion of RF/6A cells after TF overexpression with or without the Wnt signaling pathway inhibitor, an invasion assay model was used. The coculture model maintained the natural anatomic relationship between basal RPE cells and choroidal vascular endothelial cells (CECs). For the migration assay, RF/6A cells were plated in Costar Transwells (Costar, Corning, NY) with 8 µm pore-size inserts, which were put in the 24-well plates where the RPE cells had been plated. Briefly, a total of 2×10^4 ARPE-19 cells were resuspended in 600 µl fresh RPMI 1640 medium supplemented with 10% FBS and transferred into the lower chamber. Cells were incubated for 24 h at 37 °C, then transfected with TF siRNA, pEGFP-N3-hTF treated with or without Wnt signaling pathway inhibitor IWR-1-endo before 8 µm pore-size inserts were placed in the wells. Cells with no treatment served as control. Matrigel (Sigma Aldrich, Saint Louis, MO) 200 µl was added to 24-well plates and incubated at 37 °C for 30 min to form gels. A total of 2×10^4 RF/6A cells were resuspended in 200 µl fresh RPMI 1640 medium supplemented with 0.5% FBS and were placed in the upper chamber. After 48 h, the noninvading cells in the upper chambers were removed with a cotton swab, the invaded cells on the lower surface of the porous membrane were fixed with 4% paraformaldehyde for 15 min, stained with 0.1% crystal violet for 30 min, and photographed under a light microscope (Olympus, Tokyo, Japan). Five random fields (200X) were chosen in each insert, and the cell number was quantified manually. Each experiment was repeated three times.

Tube formation assay: The tube formation assay is a widely used in vitro assay to model the reorganization stage of angiogenesis [28,29]. With appropriate Matrigel support, the endothelial cells were able to form capillary-like structures (also known as tubes). A different type of coculture moldel was used to conduct the tube formation assay. Treated and untreated ARPE-19 cells were plated in Transwells with 8 µm pore-size inserts, which were put in wells where the RF/6A cells had been plated. Briefly, Matrigel was thawed and laid into 24-well culture plates to a total volume of 200 µl in each well. Plates were stored at 37 °C for 30 min to form a gel layer. After gel polymerization, 2×10^4 RF/6A cells were seeded on each well and incubated with fresh RPMI 1640 medium supplemented with 0.5% FBS for 24 h at 37 °C in humidified air with 5% CO_2. The 2×10^4 ARPE-19 cells that had been subjected to transfection for 24 h were seeded in the upper chamber. The closed networks of tubes in each well were observed with an inverted phase-contrast microscope (Olympus, Tokyo, Japan). Incomplete networks were excluded. The experiments were performed in triplicate, and five fields from each chamber were counted and averaged.

Statistical analysis: All data are expressed as mean ± standard deviation (SD) and were analyzed using the Student *t* test or one-way ANOVA. A p value of less than 0.05 was considered statistically significant.

RESULTS

Effect of $CoCl_2$ on cellular proliferation: To avoid the potential cytotoxic effect of $CoCl_2$, the MTT assay was performed to determine the optimal concentration range of $CoCl_2$ (0, 50, 100, 200, and 300 µM) in ARPE-19 cells. The MTT assay showed that ARPE-19 cell proliferation significantly

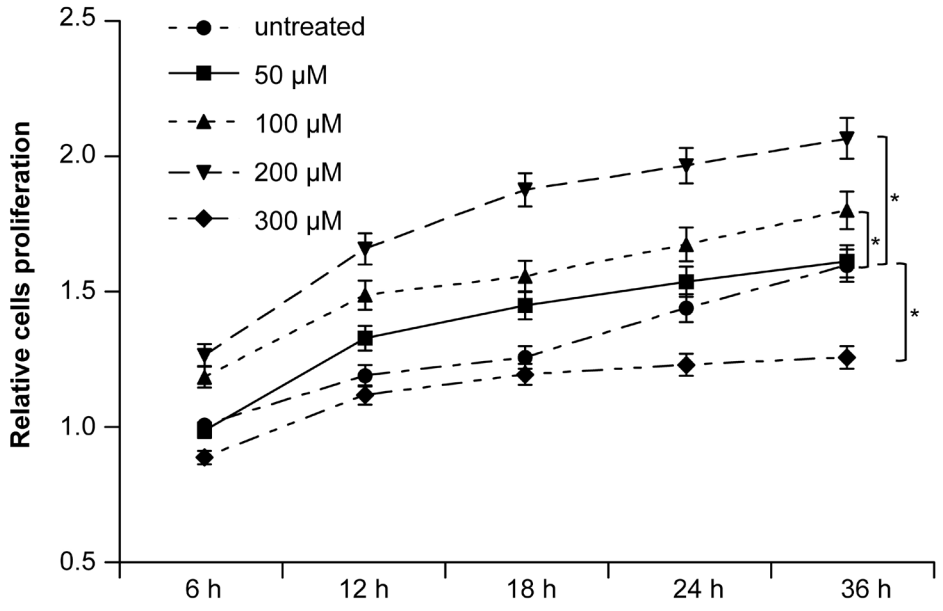

Figure 1. Analysis of effect of chemical hypoxia on the proliferation of ARPE-19 cells with MTT assay. The cell proliferation from three independent experiments is expressed as mean ± standard deviation (SD), n = 3.

increased under hypoxia at 200 μM (Figure 1), and this dose was used for the following experiments.

Upregulation of TF expression in ARPE-19 cells under hypoxic conditions: To explore the possibility that TF participates in VEGF expression under hypoxia, we investigated the effects of chemical hypoxia on the expression of TF, VEGF, and HIF-1α in ARPE-19 cells. HIF-1α has been identified as a key transcription factor that mediates increased expression of hypoxia-regulated genes such as VEGF [30]. As expected, western blotting showed that the HIF-1α protein increased over time and peaked at 12 h (Figure 2A,B). The VEGF levels in the ARPE-19 cells measured with ELISA increased consistently with HIF-1α (Figure 2C). As detected with western blotting (Figure 2A,B), TF significantly increased after 12 h of hypoxia. The results showed that TF expression was in accordance with the variations in the HIF-1α and VEGF levels (Figure 2).

TF silencing inhibits VEGF protein expression in vitro: To test the TF effect on VEGF expression in ARPE-19 cells, TF in ARPE-19 cells was knocked down by TF siRNA, and VEGF protein expression was evaluated with western blotting. TF siRNA depleted TF protein levels by 73±8% in the ARPE-19 cells (Figure 3A,B). In contrast, there was no significant difference between the cells transfected with scrambled siRNA and nontransfected cells. Accordingly, VEGF protein expression in the ARPE-19 cells was inhibited. The VEGF protein levels were downregulated by 33±3% in the ARPE-19 cells in the TF siRNA group when compared to the normal and control groups ($p<0.01$, Figure 3A,B).

Overexpression of TF upregulates VEGF expression in ARPE-19 cells: To further determine the relationship between TF and VEGF, we transfected TF plasmid into ARPE-19 cells. The TF and VEGF protein expression in the transfection group was markedly increased in ARPE-19 cells (1.92±0.08-fold and 1.71±0.11-fold, respectively) when compared to the levels in the pEGFP-N3 group and the levels in the nontransfected control cells ($p<0.01$, Figure 3C,D).

Involvement of the Wnt/β-catenin pathway in TF-induced VEGF expression: To delineate the signaling pathway underlying the observed effects of TF on ARPE-19 cells, the phosphorylation states of the signaling molecules involved in the regulation of VEGF expression were detected. Western blotting revealed that cells overexpressing human TF robustly activated the Wnt/β-catenin signaling pathway, leading to a rapid increase in the phosphorylation of GSK3β (Figure 4A,C), but reduced the phosphorylation of β-catenin and upregulated accumulation of β-catenin compared to the control groups (Figure 4A,D). IWR-1-endo is a specific inhibitor of the Wnt response [31]. IWR-1-endo stabilizes the destruction complex that consists of APC, Axin2, CK-1α, and GSK3β, increasing the level of the Axin2 protein without changing the levels of Apc or GSK3β, consequently inhibiting Wnt-induced accumulation of β-catenin. The IWR-1-exo diastereomer exhibits much less activity against the Wnt/β-catenin pathway and is used as a negative control. Notably,

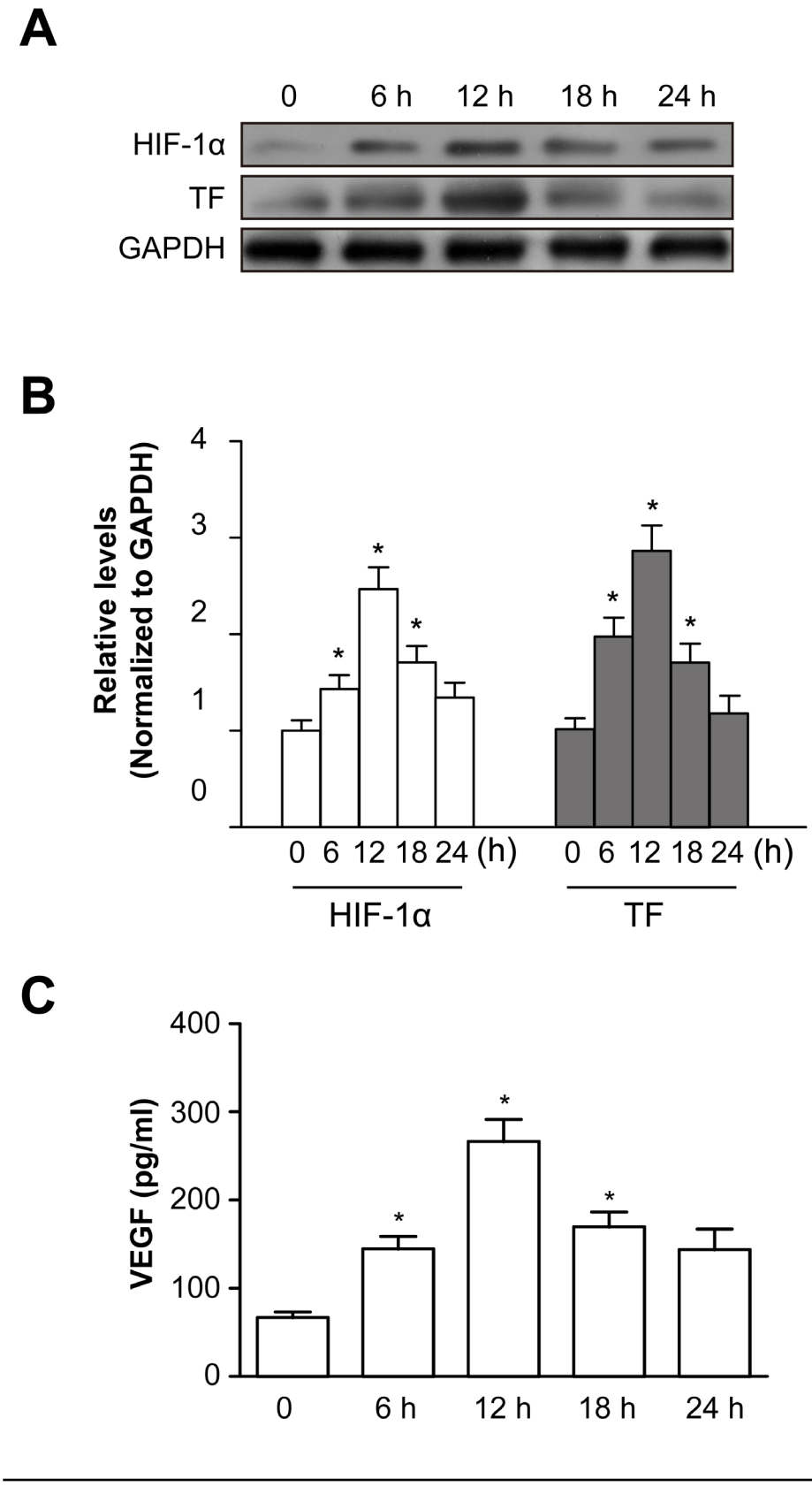

Figure 2. Chemical hypoxia induces TF, HIF-1α, and VEGF expression in ARPE-19 cells. **A**: Western blots show tissue factor (TF) and hypoxia-inducible factor 1-alpha (HIF-1α). **B**: Histogram shows the densitometric analysis of the average levels for TF and HIF-1α to glyceraldehyde 3-phosphate dehydrogenase (GAPDH) in each group. **C**: The vascular endothelial growth factor (VEGF) concentrations are examined with enzyme-linked immunosorbent assay (ELISA) at different hypoxia time points. Hypoxia significantly increased the TF, HIF-1α, and VEGF levels in the ARPE-19 cells. *p<0.05, compared with the normal control. Results are expressed as mean ± standard deviation (SD), n = 3 in each group.

we observed that IWR-1-endo changed the levels of phosphorylated GSK3β little but evidently reduced the levels of β-catenin (Figure 4C,D). The results showed that TF-induced VEGF expression was sensitive to the Wnt inhibitor IWR-1-endo, but no impact of IWR-1-exo on VEGF expression was detected. IWR-1-endo suppressed TF-induced expression of VEGF at a concentration of 10 μM (Figure 4B), suggesting that the Wnt/β-catenin signaling pathway was required for the VEGF expression in response to TF. This result indicated that VEGF was downstream of the Wnt/β-catenin pathway, which was consistent with the report that VEGF was the target gene of the Wnt/β-catenin signaling pathway [24].

Functions of RF/6A cells invasion by RPE cells in a coculture system under different TF levels: The rupture of Bruch's membrane by CECs and their migration through the extracellular matrix is an important process in the development of CNV. To determine whether TF expression from RPE influences the invasion of RF/6A cells, a non-contact coculture invading cells that over-expressed TF was significantly increased by 1.94±0.07-fold compared with the siRNA group (Figure 5).

Functions of RF/6A cells tube formation by RPE cells in a coculture system under different TF levels: Tube formation is an important function of vascular endothelial cells in angiogenesis. RF/6A cells grow in a collagen matrix gel with the culture medium of ARPE-19 cells. The coculture system showed that the TF-overexpressing ARPE-19 cells significantly increased the tube formation activity of RF/6A

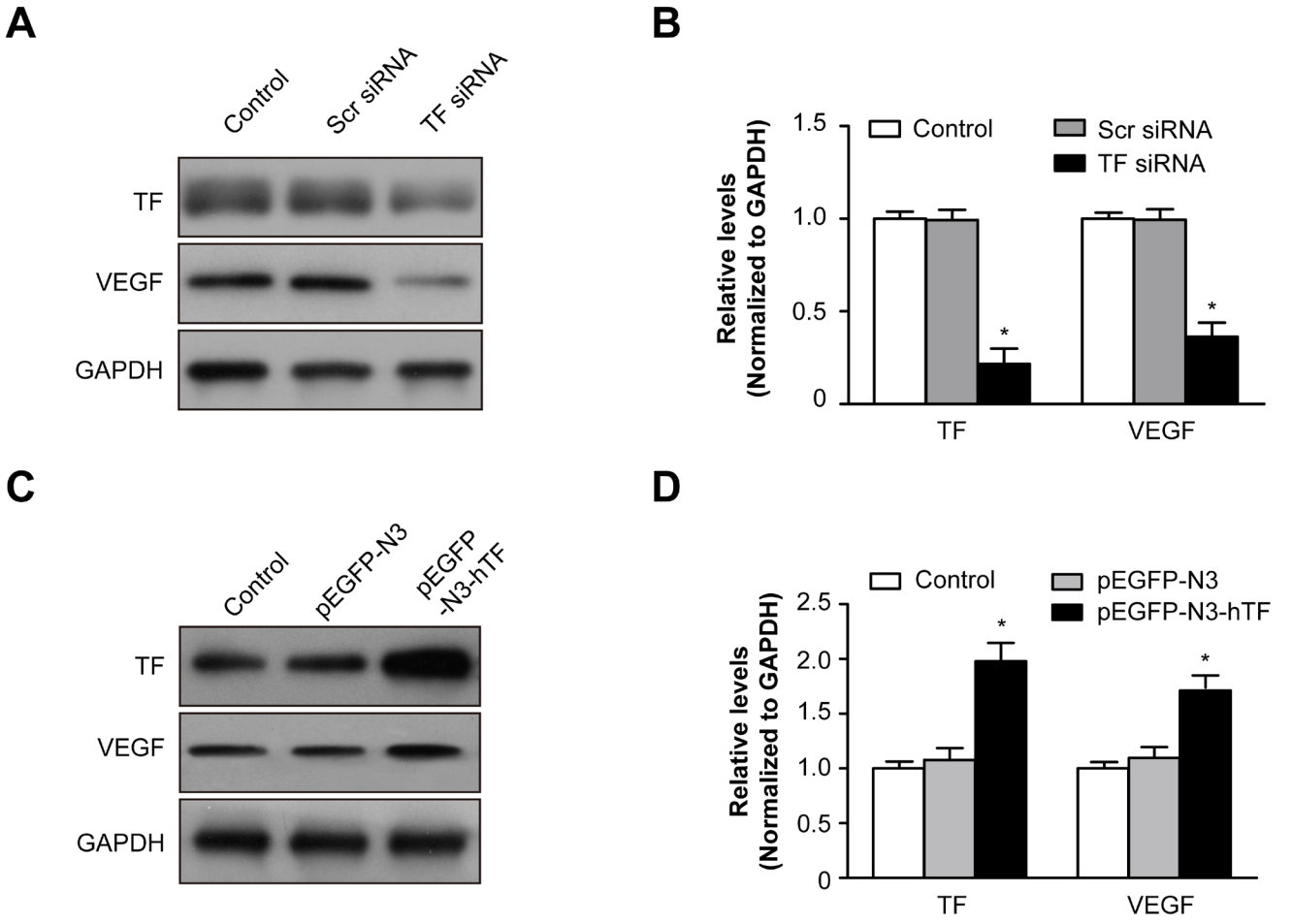

Figure 3. TF promotes VEGF expression in ARPE-19 cells. **A**: The vascular endothelial growth factor (VEGF) expression detected with western blotting in ARPE-19 cells following tissue factor (TF) siRNA transfection after 48 h. **B**: Histogram shows densitometric analysis of the average levels for TF and VEGF. Glyceraldehyde 3-phosphate dehydrogenase (GAPDH) was used as an internal control. Cells transfected with scrambled siRNA is used as negative control. **C**: Western blot analysis of VEGF expression in ARPE-19 cells after pEGFP-N3-hTF plasmid transfection after 48 h. **D**: Histogram shows densitometric analysis of the average levels for TF and VEGF. GAPDH was used as an internal control. Cells transfected with empty plasmid is used as negative control. * $p<0.01$, TF siRNA-treated group versus control groups.

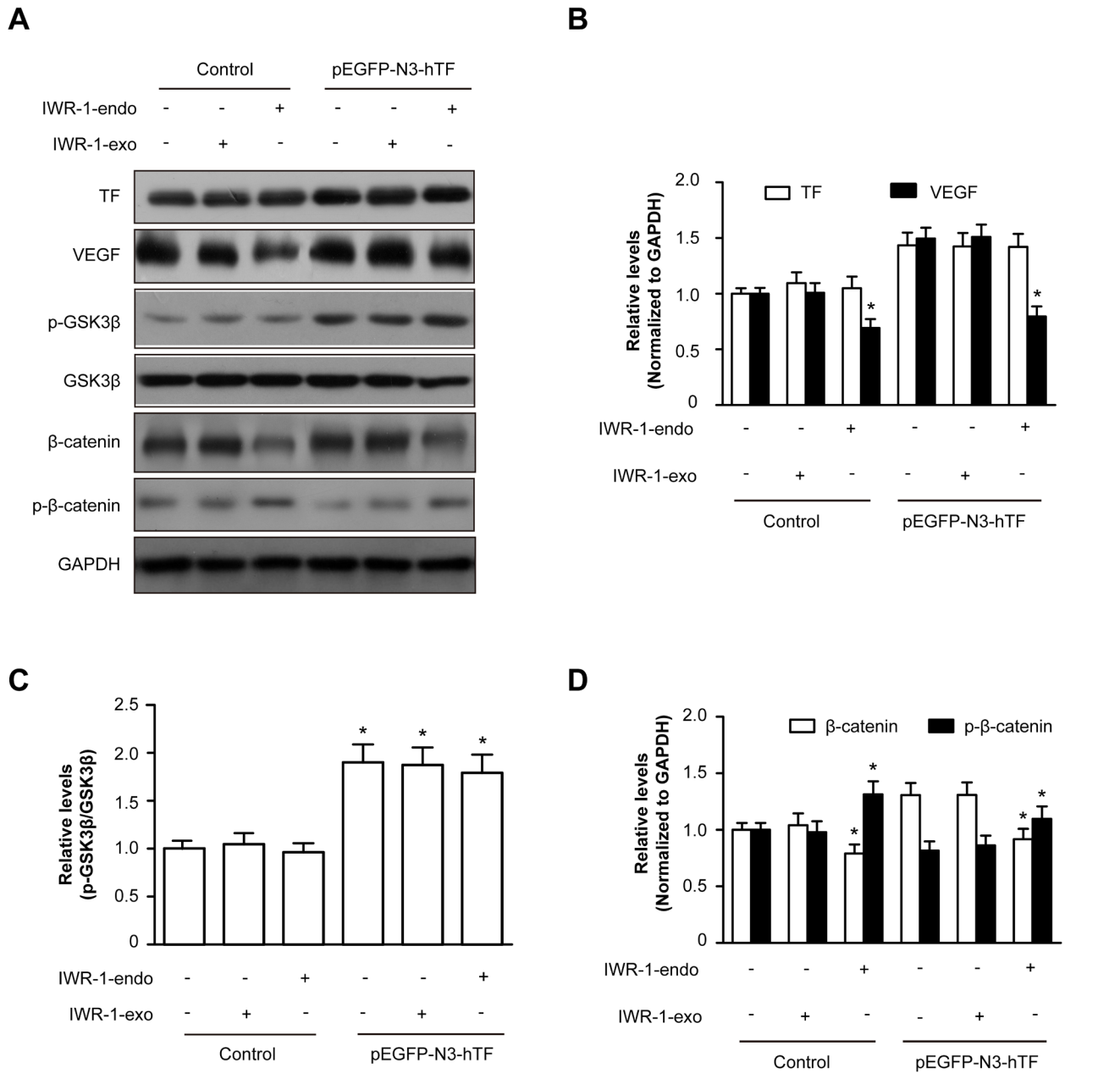

Figure 4. TF induces the activation of Wnt/β-catenin signaling pathway. **A**: Representative western blot of tissue factor (TF), vascular endothelial growth factor (VEGF), phospho-glycogen synthase kinase 3β (p-GSK3β), GSK3β, β-catenin, and p-β-catenin protein levels in ARPE-19 cells. **B**: Histograms show that TF induces VEGF expression via the Wnt/β-catenin signaling pathway. **C**, **D**: Histograms show the activation of the Wnt signaling pathway and is inhibited by IWR-1-endo. Values represent mean ± standard deviation (SD).

cells while TF siRNA showed the contrary results (Figure 6). This result indicated that TF might potentiate the VEGF-induced tube formation ability of RF/6A cells. TF induced VEGF expression and angiogenesis via the Wnt/β-catenin signaling pathway.

TF induced VEGF expression and angiogenesis via the Wnt/β-catenin signaling pathway: In order to investigate whether the Wnt/β-catenin signaling pathway participated in TF-induced VEGF expression and angiogenesis, the Wnt/β-catenin signaling pathway inhibitor IWR-1-endo was used in the Matrigel invasion and tube formation assay. When

Wnt signaling was blocked by IWR-1-endo in the ARPE-19 cells, invasiveness and tube formation were reduced significantly compared to overexpression plasmid transfected cells (Figures 5 and 6).

DISCUSSION

CNV is a major cause of blindness in humans. The pathological pathway toward CNV begins with the breakdown of Bruch's membrane, resulting in local ischemia and hypoxia. The condition of CNV is stimulated by one or more angiogenic factors, particularly VEGF under hypoxic or inflammatory conditions [32]. Then the CECs are activated and transmigrate toward or across the RPE into the neurosensory retina, where the CECs proliferate into new vessels [33]. Our previous study showed that TF-siRNA substantially inhibited the proliferation and migration of human umbilical vein endothelial cells (HUVECs) [19].

Angiogenesis is a complex process involving vascular endothelial cell proliferation, migration, and tube formation [34]. RF/6A, which is a choroid–retinal endothelial cell line, is widely used for in vitro studies on retinal and choroidal neovascularization [35,36]. In the present study, we used the RF/6A cell line to imitate the process of neovascularization.

In a mice model of laser-induced CNV, we found that TF played an important role in CNV formation, and the anti-TF monoclonal antibody significantly decreased leakage in CNV lesions. After anti-TF monoclonal antibody treatment, the TF levels of the RPE–choroid complexes and the retina were decreased. Surprisingly, VEGF expression revealed a similar change [20], while the signal mechanism involved in the effect of TF on VEGF is unknown.

To further explore the regulation of TF on VEGF and the possible signaling pathways, TF expression was changed by transfection of siRNA or overexpression of plasmids in the ARPE-19 cells. We demonstrated that TF siRNA specifically knocked down TF expression in ARPE-19 cells, and VEGF protein levels decreased accordingly. In contrast, TF overexpression upregulated VEGF expression (Figure 3). Western blotting was conducted to evaluate the protein phosphorylation changes regulated by TF. The phosphoprotein results indicated that TF regulates activation of the Wnt/β-catenin signaling pathway, participating in the expression of VEGF (Figure 4). The specific inhibitor of the Wnt/β-catenin pathway IWR-1-endo inhibited the effect on VEGF expression. Silencing endogenous TF significantly suppressed the Wnt/β-catenin signal transduction cascades. Therefore, the regulation of TF on VEGF expression may be mediated by

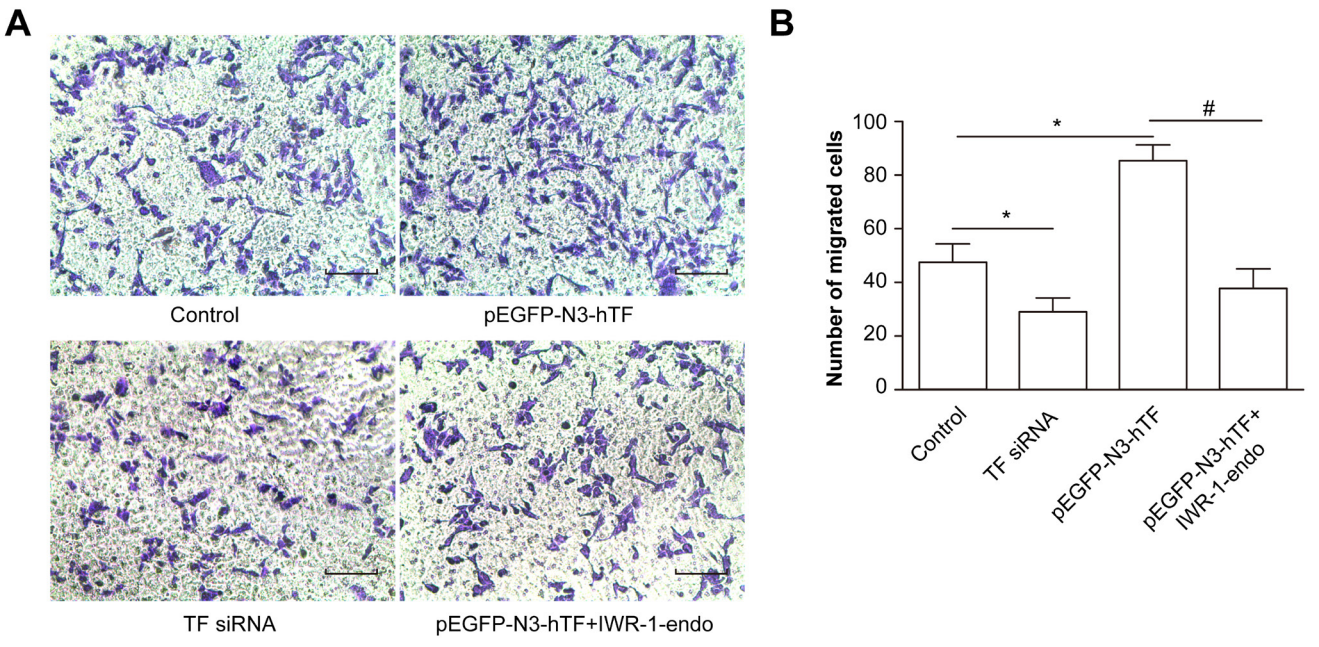

Figure 5. Impact of RF/6A cell invasion by TF expression in ARPE-19 cells. **A**: Representative photographs of invasive RF/6A cells in each group (200X magnification). **B**: The average number of invasive RF/6A cells per field. *p<0.01, tissue factor (TF) siRNA versus Control. Overexpression of TF greatly increased the number of invasive cells (*p<0.01, pEGFP-N3-hTF versus Control), and this effect was significantly reduced with the Wnt inhibitor (#p<0.01, pEGFP-N3-hTF versus pEGFP-N3-hTF+IWR-1-endo). Bar = 50 μm.

activation of the Wnt/β-catenin signaling pathway, but the detailed mechanism requires further exploration.

We demonstrated that TF could effectively promote VEGF-induced choroid-retinal endothelial cell migration and tube formation, which is mediated by the Wnt/β-catenin signaling pathway (Figure 5 and Figure 6). We investigated several signaling pathways in our study such as PI3K/Akt, but did not find statistical significance. In addition, p38 MAPK signaling pathway is in the upstream of TF. We chose the Wnt/β-catenin pathway instead of the others because VEGF was found to be a target gene of β-catenin while TF was not [24]. Multiple signaling pathways might exist in TF-overexpressing RPE cells. However, the Wnt pathway seems to be upregulated and is a significant pathway of this regulation in the present study. One of the most upregulated phosphoproteins in TF-overexpressed ARPE-19 cells is GSK3β. In the canonical Wnt signaling pathway, serine 9 of GSK3β is rapidly phosphorylated, resulting in inhibition of GSK3β kinase activity, mediating proteasomal targeting and triggering a rapid accumulation of nuclear β-catenin. Badimon and his colleagues [37] revealed that the Wnt pathway is concerned with TF-silenced human vascular smooth muscle cell (HVSMC) polarization and cell motility. These results demonstrated that TF promoted RF/6A cell invasion and tube formation by transcriptionally upregulating VEGF involving activation of the Wnt/β-catenin signaling pathway. In vivo relationships between TF and VEGF will be investigated in further work.

TF signaling has been linked to TF cytoplasmic domain phosphorylation [17,38], especially phosphorylation of the three serine residues (Ser253, Ser258, and Ser263) [39]. Several studies suggested that phosphorylation of the TF cytoplasmic domain results in activation of various MAPK family members and triggers gene transcription [40-42]. However, some investigators have found that deletion of the cytoplasmic tail of full-length TF does not result in abnormal angiogenesis [43]. Arderiu et al. [44] showed that the lack of a cytoplasmic domain does not abrogate TF signaling through Akt although other studies showed that the cytoplasmic tail of TF plays an important role in the regulation of VEGF expression and angiogenesis in tumor growth [45-47]. Thus, it is necessary to explore how TF activates the Wnt/β-catenin signaling pathway or which member of the Wnt family interacts with TF.

In conclusion, our study indicated that TF and VEGF might coordinate in the formation of CNV. Silencing TF expression in RPE cells inhibited VEGF expression, while

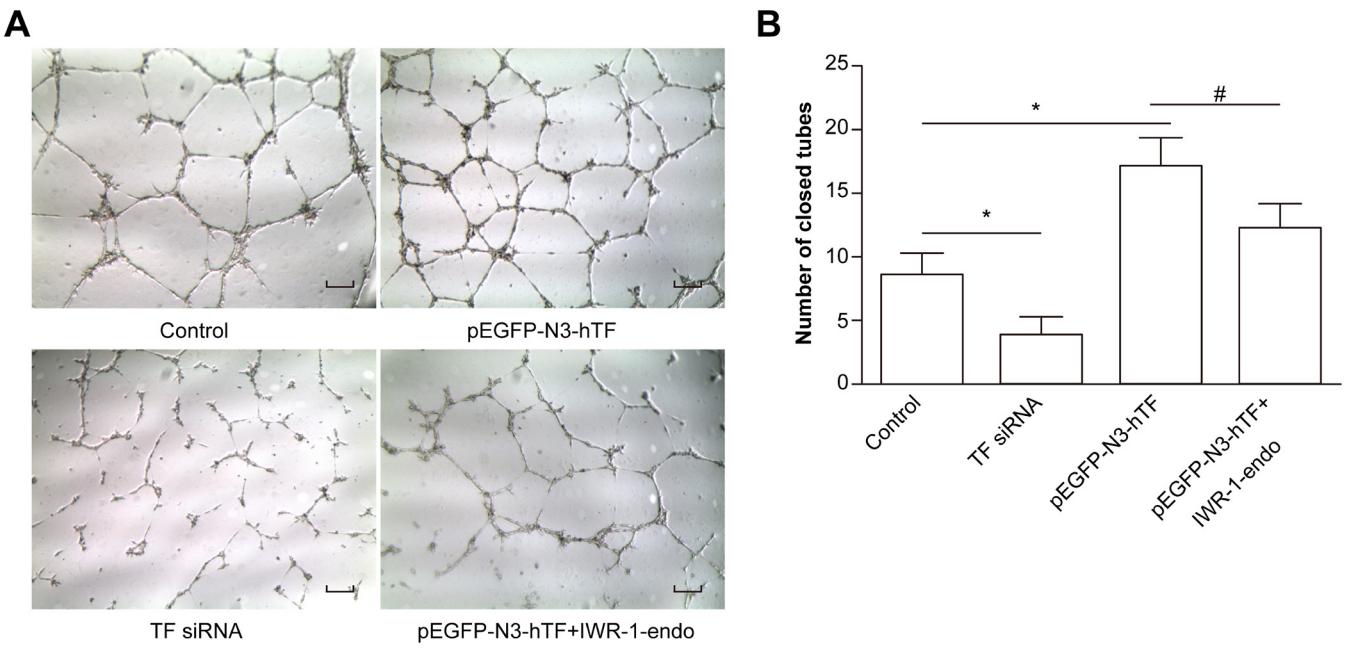

Figure 6. Impact of RF/6A cell tube formation by TF expression in ARPE-19 cells. **A**: Representative photographs of tube formation in each group (40X magnification). **B**: The average number of closed networks of tubes per field. Silence of tissue factor (TF) greatly reduced the tube formation of cocultured RF/6A cells (*p<0.01, TF siRNA versus Control). Overexpression of TF greatly increased the tube formation of cocultured RF/6A cells (*p<0.01, pEGFP-N3-hTF versus Control), and this effect was significantly reduced with the Wnt inhibitor (#p<0.01, pEGFP-N3-hTF versus pEGFP-N3-hTF+IWR-1-endo). Bar = 100 µm.

overexpression of TF in the RPE cells resulted in increased VEGF expression, suggesting VEGF was positively regulated by TF in vitro. TF promotes choroidal–retina vascular endothelial cell invasion and tube formation by upregulating VEGF. TF signals through the Wnt/β-catenin pathway to regulate VEGF and vascular formation. We anticipate that targeted therapy toward TF and Wnt signaling and its downstream proteins might be promising for interventions of pathological processes involving TF-regulated angiogenesis and inflammation. Future experiments in more relevant model systems are needed to clear the way toward clinical application of this novel finding.

APPENDIX 1. STR ANALYSIS.

To access the data, click or select the words "Appendix 1."

ACKNOWLEDGMENTS

The study was supported by National Natural Science Foundation of China (81,200,680).

REFERENCES

1. Finger RP, Fimmers R, Holz FG, Scholl HP. Prevalence and causes of registered blindness in the largest federal state of Germany. Br J Ophthalmol 2011; 95:1061-7. [PMID: 21378005].
2. Takata S, Masuda T, Nakamura S, Kuchimaru T, Tsuruma K, Shimazawa M, Nagasawa H. kizaka-Kondoh S, Hara H. The effect of triamcinolone acetonide on laser-induced choroidal neovascularization in mice using a hypoxia visualization bioimaging probe. Sci Rep 2015; 5:9898-[PMID: 25927172].
3. Kwak N, Okamoto N, Wood JM, Campochiaro PA. VEGF is major stimulator in model of choroidal neovascularization. Invest Ophthalmol Vis Sci 2000; 41:3158-64. [PMID: 10967078].
4. Brown DM, Kaiser PK, Michels M, Soubrane G, Heier JS, Kim RY, Sy JP, Schneider S. Ranibizumab versus verteporfin for neovascular age-related macular degeneration. N Engl J Med 2006; 355:1432-44. [PMID: 17021319].
5. Rosenfeld PJ, Brown DM, Heier JS, Boyer DS, Kaiser PK, Chung CY, Kim RY. Ranibizumab for neovascular age-related macular degeneration. N Engl J Med 2006; 355:1419-31. [PMID: 17021318].
6. Saint-Geniez M, Maharaj AS, Walshe TE, Tucker BA, Sekiyama E, Kurihara T, Darland DC, Young MJ, D'Amore PA. Endogenous VEGF is required for visual function: evidence for a survival role on muller cells and photoreceptors. PLoS One 2008; 3:e3554-[PMID: 18978936].
7. Bach RR. Initiation of coagulation by tissue factor. CRC Crit Rev Biochem 1988; 23:339-68. [PMID: 3067973].
8. Cho Y, Cao X, Shen D, Tuo J, Parver LM, Rickles FR, Chan CC. Evidence for enhanced tissue factor expression in age-related macular degeneration. Lab Invest 2011; 91:519-26. [PMID: 21042291].
9. Chu AJ. Tissue factor upregulation drives a thrombosis-inflammation circuit in relation to cardiovascular complications. Cell Biochem Funct 2006; 24:173-92. [PMID: 15617024].
10. Carmeliet P, Mackman N, Moons L, Luther T, Gressens P, Van Vlaenderen I, Demunck H, Kasper M, Breier G, Evrard P, Muller M, Risau W, Edgington T, Collen D. Role of tissue factor in embryonic blood vessel development. Nature 1996; 383:73-5. [PMID: 8779717].
11. Grossniklaus HE, Ling JX, Wallace TM, Dithmar S, Lawson DH, Cohen C, Elner VM, Elner SG, Sternberg P Jr. Macrophage and retinal pigment epithelium expression of angiogenic cytokines in choroidal neovascularization. Mol Vis 2002; 8:119-26. [PMID: 11979237].
12. Al-Latayfeh M, Silva PS, Sun JK, Aiello LP. Antiangiogenic therapy for ischemic retinopathies. Cold Spring Harb Perspect Med 2012; 2:a006411-[PMID: 22675660].
13. Bhutto IA, Baba T, Merges C, Juriasinghani V, McLeod DS, Lutty GA. C-reactive protein and complement factor H in aged human eyes and eyes with age-related macular degeneration. Br J Ophthalmol 2011; 95:1323-30. [PMID: 21633121].
14. Kolomeyer AM, Sugino IK, Zarbin MA. Characterization of conditioned media collected from aged versus young human eye cups. Invest Ophthalmol Vis Sci 2011; 52:5963-72. [PMID: 21398279].
15. Medearis S, Han IC, Huang JK, Yang P, Jaffe GJ. The role of Bcl-xL in mouse RPE cell survival. Invest Ophthalmol Vis Sci 2011; 52:6545-51. [PMID: 21724914].
16. Liu XC, Liu XF, Jian CX, Li CJ, He SZ. IL-33 is induced by amyloid-beta stimulation and regulates inflammatory cytokine production in retinal pigment epithelium cells. Inflammation 2012; 35:776-84. [PMID: 21898270].
17. Belting M, Dorrell MI, Sandgren S, Aguilar E, Ahamed J, Dorfleutner A, Carmeliet P, Mueller BM, Friedlander M, Ruf W. Regulation of angiogenesis by tissue factor cytoplasmic domain signaling. Nat Med 2004; 10:502-9. [PMID: 15098027].
18. Carneiro-Lobo TC, Lima MT, Mariano-Oliveira A, Dutra-Oliveira A, Oba-Shinjo SM, Marie SK, Sogayar MC, Monteiro RQ. Expression of tissue factor signaling pathway elements correlates with the production of vascular endothelial growth factor and interleukin-8 in human astrocytoma patients. Oncol Rep 2014; 31:679-86. [PMID: 24297570].
19. Peng W, Yu Y, Li T, Zhu Y, Chen H. The effects of small interfering RNA-targeting tissue factor on an in vitro model of neovascularization. Mol Vis 2013; 19:1296-303. [PMID: 23805036].
20. Wang L, Yang Z, Yu Y, Cui C, Guan H, Chen H. Blockage of tissue factor ameliorates the lesion of laser-induced choroidal neovascularization in mice. Exp Eye Res 2014; 127:117-23. [PMID: 25063201].
21. Miller JR. The Wnts. Genome Biol 2002; 3:xxx-.

22. Nusse R. Wnt signaling in disease and in development. Cell Res 2005; 15:28-32. [PMID: 15686623].

23. MacDonald BT, Tamai K, He X. Wnt/beta-catenin signaling: components, mechanisms, and diseases. Dev Cell 2009; 17:9-26. [PMID: 19619488].

24. Lichtlen P, Lam TT, Nork TM, Streit T, Urech DM. Relative contribution of VEGF and TNF-alpha in the cynomolgus laser-induced CNV model: comparing the efficacy of bevacizumab, adalimumab, and ESBA105. Invest Ophthalmol Vis Sci 2010; 51:4738-45. [PMID: 20393113].

25. Hu Y, Chen Y, Lin M, Lee K, Mott RA, Ma JX. Pathogenic role of the Wnt signaling pathway activation in laser-induced choroidal neovascularization. Invest Ophthalmol Vis Sci 2013; 54:141-54. [PMID: 23211829].

26. Katoh Y, Katoh M. Comparative integromics on VEGF family members. Int J Oncol 2006; 28:1585-9. [PMID: 16685460].

27. Zhang X, Gaspard JP, Chung DC. Regulation of vascular endothelial growth factor by the Wnt and K-ras pathways in colonic neoplasia. Cancer Res 2001; 61:6050-4. [PMID: 11507052].

28. Zhu J, Wang YS, Zhang J, Zhao W, Yang XM, Li X, Jiang TS, Yao LB. Focal adhesion kinase signaling pathway participates in the formation of choroidal neovascularization and regulates the proliferation and migration of choroidal microvascular endothelial cells by acting through HIF-1 and VEGF expression in RPE cells. Exp Eye Res 2009; 88:910-8. [PMID: 19111720].

29. Feng YF, Guo H, Yuan F, Shen MQ. Lipopolysaccharide Promotes Choroidal Neovascularization by Up-Regulation of CXCR4 and CXCR7 Expression in Choroid Endothelial Cell. PLoS One 2015; 10:e0136175-[PMID: 26288180].

30. Zhang ZX, Wang YS, Shi YY, Hou HY, Zhang C, Cai Y, Dou GR, Yao LB, Li FY. Hypoxia specific SDF-1 expression by retinal pigment epithelium initiates bone marrow-derived cells to participate in Choroidal neovascularization in a laser-induced mouse model. Curr Eye Res 2011; 36:838-49. [PMID: 21851170].

31. Chen B, Dodge ME, Tang W, Lu J, Ma Z, Fan CW, Wei S, Hao W, Kilgore J, Williams NS, Roth MG, Amatruda JF, Chen C, Lum L. Small molecule-mediated disruption of Wnt-dependent signaling in tissue regeneration and cancer. Nat Chem Biol 2009; 5:100-7. [PMID: 19125156].

32. Bai Y, Zhao M, Zhang C, Li S, Qi Y, Wang B, Huang L, Li X. Anti-angiogenic effects of a mutant endostatin: a new prospect for treating retinal and choroidal neovascularization. PLoS One 2014; 9:e112448-[PMID: 25380141].

33. Skeie JM, Mullins RF. Elastin-mediated choroidal endothelial cell migration: possible role in age-related macular degeneration. Invest Ophthalmol Vis Sci 2008; 49:5574-80. [PMID: 18708613].

34. Liu X, Zhao D, James L, Li J, Zeng H. Requirement of the nuclear localization of transcription enhancer factor 3 for proliferation, migration, tube formation, and angiogenesis induced by vascular endothelial growth factor. FASEB J 2011; 25:1188-97. [PMID: 21169383].

35. Kasai A, Shintani N, Oda M, Kakuda M, Hashimoto H, Matsuda T, Hinuma S, Baba A. Apelin is a novel angiogenic factor in retinal endothelial cells. Biochem Biophys Res Commun 2004; 325:395-400. [PMID: 15530405].

36. Ottino P, Finley J, Rojo E, Ottlecz A, Lambrou GN, Bazan HE, Bazan NG. Hypoxia activates matrix metalloproteinase expression and the VEGF system in monkey choroid-retinal endothelial cells: Involvement of cytosolic phospholipase A2 activity. Mol Vis 2004; 10:341-50. [PMID: 15162095].

37. Pena E, Arderiu G, Badimon L. Tissue factor induces human coronary artery smooth muscle cell motility through Wnt-signalling. J Thromb Haemost 2013; 11:1880-91. [PMID: 23782925].

38. van den Berg YW, van den Hengel LG, Myers HR, Ayachi O, Jordanova E, Ruf W, Spek CA, Reitsma PH, Bogdanov VY, Versteeg HH. Alternatively spliced tissue factor induces angiogenesis through integrin ligation. Proc Natl Acad Sci USA 2009; 106:19497-502. [PMID: 19875693].

39. Zioncheck TF, Roy S, Vehar GA. The cytoplasmic domain of tissue factor is phosphorylated by a protein kinase C-dependent mechanism. J Biol Chem 1992; 267:3561-4. [PMID: 1740409].

40. Ott I, Weigand B, Michl R, Seitz I, Sabbari-Erfani N, Neumann FJ, Schomig A. Tissue factor cytoplasmic domain stimulates migration by activation of the GTPase Rac1 and the mitogen-activated protein kinase p38. Circulation 2005; 111:349-55. [PMID: 15642762].

41. Ossoli A, Remaley AT, Vaisman B, Calabresi L, Gomaraschi M. Plasma-derived and synthetic high density lipoproteins inhibit tissue factor in endothelial cells and monocytes. Biochem J 2016; 473:211-9. [PMID: 26556891].

42. Dong R, Chen W, Feng W, Xia C, Hu D, Zhang Y, Yang Y, Wang DW, Xu X, Tu L. Exogenous Bradykinin Inhibits Tissue Factor Induction and Deep Vein Thrombosis via Activating the eNOS/Phosphoinositide 3-Kinase/Akt Signaling Pathway. Cell Physiol Biochem 2015; 37:1592-606. [PMID: 26517864].

43. Versteeg HH, Sorensen BB, Slofstra SH, Van den Brande JH, Stam JC. van Bergen en Henegouwen PM, Richel DJ, Petersen LC, Peppelenbosch MP. VIIa/tissue factor interaction results in a tissue factor cytoplasmic domain-independent activation of protein synthesis, p70, and p90 S6 kinase phosphorylation. J Biol Chem 2002; 277:27065-72. [PMID: 12019261].

44. Arderiu G, Pena E, Aledo R, Badimon L. Tissue factor-Akt signaling triggers microvessel formation. J Thromb Haemost 2012; 10:1895-905. [PMID: 22784289].

45. Abe K, Shoji M, Chen J, Bierhaus A, Danave I, Micko C, Casper K, Dillehay DL, Nawroth PP, Rickles FR. Regulation of vascular endothelial growth factor production and angiogenesis by the cytoplasmic tail of tissue factor. Proc Natl Acad Sci USA 1999; 96:8663-8. [PMID: 10411932].

46. Rickles FR, Shoji M, Abe K. The role of the hemostatic system in tumor growth, metastasis, and angiogenesis: tissue factor is a bifunctional molecule capable of inducing both fibrin deposition and angiogenesis in cancer. Int J Hematol 2001; 73:145-50. [PMID: 11372724].

47. Paborsky LR, Caras IW, Fisher KL, Gorman CM. Lipid association, but not the transmembrane domain, is required for tissue factor activity. Substitution of the transmembrane domain with a phosphatidylinositol anchor. J Biol Chem 1991; 266:21911-6. [PMID: 1834663].

Articles are provided courtesy of Emory University and the Zhongshan Ophthalmic Center, Sun Yat-sen University, P.R. China. The print version of this article was created on 25 July 2016. This reflects all typographical corrections and errata to the article through that date. Details of any changes may be found in the online version of the article.